

Impulse-driven Capsule by Coil-induced Magnetic Field Implementation

Takahiro Ito *

Toin University of Yokohama,
Kanagawa, Japan

Takuto Ogushi †

Toin University of Yokohama,
Kanagawa, Japan

Teru Hayashi ‡

Ogasawara Precision Laboratory,
Kanagawa, Japan

Abstract— We have developed a traveling small capsule, which has a smooth outer surface and is driven by inertia force and friction force. Measuring only 7 mm in diameter and 12 mm in length, it is sufficiently small to be placed in the human gullet or intestines. The capsule contains a small magnet and a coil, and an electric pulse drives the magnet to move the capsule. To investigate the feasibility of our traveling capsule, we conducted theoretical analyses using a simple model. Separating the phenomena into four steps, we obtained fundamental equations and clarified the motion. We performed an experimental investigation on making our capsule travel on a plastic material, which has similar elasticity characteristics to the living body. We also showed that it can travel on the surface of a pig's intestine. We measured the temperature of the capsule during its movement to evaluate safety for the human body. Using the calculated results, we created a new input signal pattern for the capsule and thus successfully doubled the speed of movement of the capsule. Our capsule may be useful for medical treatments such as inspection, drug delivery and operation.

Keywords: micromechanism, friction force, magnetic force

I. Introduction

Seventy percent of the human body is composed of soft tubes with diameter ranging from μm order to cm order. Therefore, capsules which can travel inside these tubes are useful for medical treatments such as inspection, drug delivery and operation. Various kinds of machines for this purpose have been proposed [1] but most of them had hands in order to crawl in tubes [2],[3],[4],[5],[6]. However, the outer surface of the machine should not have any projections so as not to injure the surrounding site. Machines that have a smooth outer surface and crawl have been developed. Among them, some utilized a fluid actuator to move [7],[8], but it was more than 30 mm long and needed a high-power fluid pump. To avoid using legs or hands to crawl, eel-like mechanisms were theoretically analyzed [9],[10], and inchworm-type robots were developed [11], but they had relatively complicated mechanisms and it was difficult to make them as small as medicine tablets. This paper describes a traveling small

capsule, which has a smooth surface and is driven by inertia force and friction force. Measuring only 7 mm in diameter and 12 mm in length, our capsule is sufficiently small to be placed in the human gullet or intestines. In this paper, we present a theoretical analysis to show how the capsule travels with a simple mechanism, and evaluate the results of experiments to improve its traveling capability.

II. Theoretical analysis

Structure and principle of the traveling capsule

Our capsule travels by a to-and-fro motion of an inner mass. The capsule consists of the body (M) with coil and the moving mass (m) as shown in Fig. 1. The coil is made by 200 turns of ϕ 0.05 mm copper. The moving mass is an Nd-Fe-B permanent magnet and is driven by magnetic force f_m by applying a step-shaped current to the coil. The outside appearance of the capsule is shown in Fig. 2.

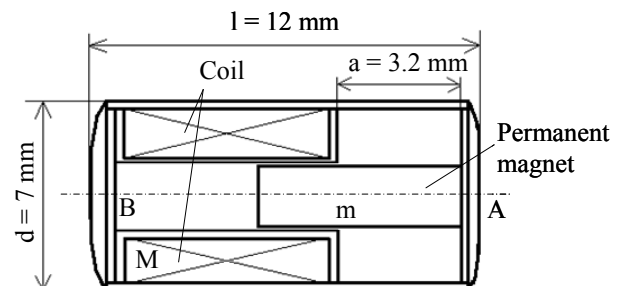


Fig. 1. Schematic illustration of the capsule (cross section).

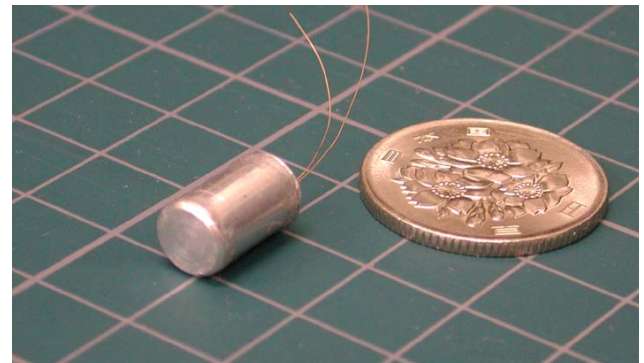


Fig. 2. Photograph of the traveling capsule.

*E-mail: t-ito@cc.toin.ac.jp

† E-mail: t17i010@edu.toin.ac.jp

‡ E-mail: t-hayashi@ogswr-pl.co.jp

The physical model of the capsule is shown in Fig. 3. The movement of mass m is restricted between two stoppers A and B. The resistance force f_r acts against the movement of the body M from the base. For simplicity, we neglected the friction force between m and M , which is relatively very small and does not play a major role in propelling the capsule. For the theoretical analysis, the motion of the capsule is divided into the following four steps.

Step 1: As shown in Fig. 3 (i), M and m pull each other by magnetic force f_m . The mass m that starts from stopper A is accelerated by the magnetic force f_m and also the body M is accelerated by the force $(f_m - f_r)$ until m collides with M at stopper B. Defining that M moves by distance x_0 to right side and m u_0 to left side in time t_0 by that motion, we will be able to determine these values.

Step 2: As shown in Fig. 3 (ii), we assume that after collision, M and m move together with initial velocity v_0 , are decelerated by friction force f_r and finally come to a stop. Defining that M and m move by x_1 to the left within time t_1 by the motion shown in Fig. 3 (iii), we can determine these values.

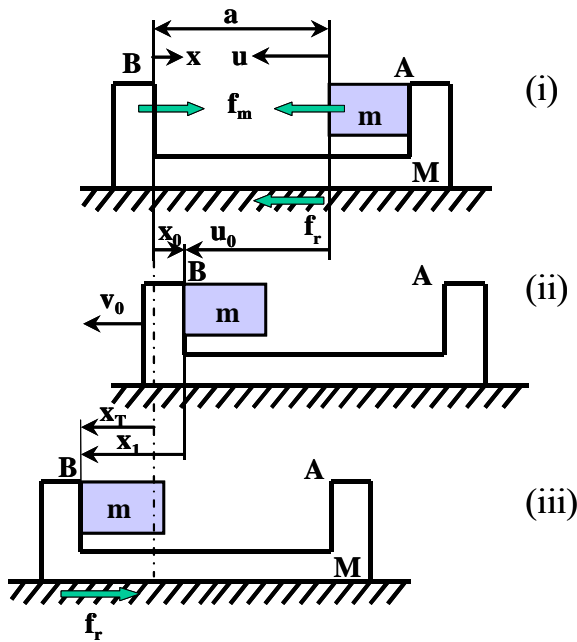


Fig. 3. Traveling mechanism of the capsule.

Step 3: Like Step 1, upon applying magnetic force $-f_m'$ by adding a (-) step-shaped current to the coil, M and m push each other. The mass m that starts from stopper B is accelerated by magnetic force f_m' and also the body M is accelerated by the force $(f_m' - f_r)$ until m collides with M at stopper A. Defining that M moves by distance x_0' to the left within time t_0' in that motion, we can determine these values.

Step 4: Like Step 2, M and m move together with initial

velocity v_0' , are decelerated by friction force f_r and then come to a stop. Defining that M and m move by x_1' to the right within t_1' in that motion, we can determine these values.

As a result, defining that the body M moves x_T to the left within time t_T , they will be expressed by the following two equations:

$$x_T = (x_1 - x_0) - (x_1' - x_0') \quad (1)$$

$$t_T = t_0 + t_1 + t_0' + t_1' \quad (2)$$

In the design, we should aim to increase the value of x_T and decrease the value of t_T .

Equations of capsule motion

We can obtain equations of motion in each step as follows:

Step 1: We define that x and u are displacements of M and m respectively, and that a is the total gap between the moving mass and stoppers. For M and m , equations of motion are expressed by,

$$M \cdot \ddot{x} + f_r = f_m \quad (3)$$

$$m \cdot \ddot{u} = f_m \quad (4)$$

Actually, magnetic force f_m varies depending on the displacement x , u but for simplicity, we set f_m to be constant as an approximation.

From equations (3) and (4), the velocities \dot{x} , \dot{u} and the displacements x , u become as follows:

$$\dot{x} = \frac{f_m - f_r}{M} \cdot t, \quad x = \frac{f_m - f_r}{M} \cdot \frac{t^2}{2} \quad (5)$$

$$\dot{u} = \frac{f_m}{m} \cdot t, \quad u = \frac{f_m}{m} \cdot \frac{t^2}{2} \quad (6)$$

As collision occurs when $x + u = a$, the time t_0 and the displacement x_0 at that moment become,

$$t_0 = \frac{1}{\sqrt{(n+1)f-1}} K_t, \quad K_t = \sqrt{\frac{2aM}{f_r}} \quad (7)$$

$$x_0 = \frac{f-1}{(n+1)f-1} a \quad (8)$$

where the mass ratio n and force ratio f are defined as follows:

$$n = \frac{M}{m} \quad \text{and} \quad f = \frac{f_m}{f_r} \quad (9)$$

Step 2: Assuming that the collision is inelastic, that is, the coefficient of restitution $e = 0$, the initial velocity v_0 of the body (combined mass $M+m$) is expressed as follows:

$$v_0 = \left(\frac{m \cdot \dot{u} - M \cdot \dot{x}}{M + m} \right)_{t=t_0} = \frac{n}{(n+1)\sqrt{(n+1)f-1}} \sqrt{\frac{2af_r}{M}} \quad (10)$$

Therefore, the equation of motion for the combined mass becomes,

$$(M + m)\ddot{x} + f_r = 0, \quad (\dot{x})_{t=0} = v_0 \quad (11)$$

Solving the above equation,

$$\dot{x} = v_0 - \frac{f_r}{M + m} \cdot t, \quad x = v_0 t - \frac{f_r}{M + m} \cdot \frac{t^2}{2} \quad (12)$$

As the combined mass moves until $\dot{x} = 0$, the time t_1 and displacement x_1 at this moment are expressed as follows:

$$t_1 = \frac{1}{\sqrt{(n+1)f-1}} \sqrt{\frac{2aM}{f_r}} \quad (13)$$

$$x_1 = \frac{n}{(n+1)\{(n+1)f-1\}} a \quad (14)$$

Step 3: Similar equations as used in Step 1 can be used. However, the direction of motion x is reversed and the value of driving force f_m' must be different from f_m , so the values of t_0' and x_0' are obtained as follows:

$$t_0' = \frac{1}{\sqrt{(n+1)f'-1}} \sqrt{\frac{2aM}{f_r'}} \quad (15)$$

$$x_0' = -\frac{f'-1}{(n+1)f'-1} a \quad (16)$$

Step 4: Similar equations as used in Step 2 can be used. Changing the direction of x and changing f_m to f_m' , the values of t_1' and x_1' are obtained as follows:

$$t_1' = \frac{1}{\sqrt{(n+1)f'-1}} \sqrt{\frac{2aM}{f_r'}} \quad (17)$$

$$x_1' = -\frac{n}{(n+1)\{(n+1)f'-1\}} a \quad (18)$$

The motions obtained from these equations are summarized in Fig. 4.

Examination of the theoretical analysis

The following important results are derived from the above theoretical analysis.

(1) Regarding the period, stroke x_T is expressed by the following equations:

$$x_T = \Delta x - \Delta x', \quad \Delta x' = \Delta x(f \rightarrow f') \quad (19)$$

$$\Delta x = C_x \cdot a, \quad C_x = \frac{(2n+1)-(n+1)f}{(n+1)\{(n+1)f-1\}} \quad (20)$$

(2) Regarding the period t_T for a stroke,

$$t_T = \Delta t + \Delta t', \quad \Delta t' = \Delta t(f \rightarrow f') \quad (21)$$

$$\Delta t = C_t \cdot K_t, \quad C_t = \frac{2}{\sqrt{(n+1)f-1}} \quad (22)$$

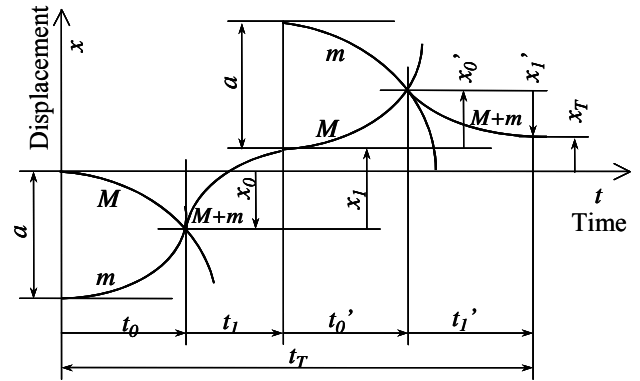


Fig. 4. Summary of result of analyzed motion.

(3) The traveling speed is the most important factor when designing the traveling capsule. From the above analysis, it is clear that one stroke motion of inner mass m dominates the total speed. To see the tendency of the force–speed relation, one stroke motion is considered first as follows. The equations for traveling speed S are expressed as follows:

$$S = \frac{\Delta x}{\Delta t} = C_s \cdot K_s \quad (23)$$

$$C_s = \frac{C_x}{C_t} = \frac{(2n+1)-(n+1)f}{2(n+1)\sqrt{(n+1)f-1}}, \quad K_s = \sqrt{\frac{a \cdot f_r}{2M}} \quad (24)$$

The effect of n and f on the coefficient of traveling speed C_s is summarized in Fig. 5. In the figure, force ratio $f (= f_m/f_r)$ should be greater than 1, because friction force between the capsule and the base cannot be greater than magnetic force f_m while the capsule is moving. From the figure, it is found that we can choose the parameters as follows to design the high-speed capsule:

- (a) Mass ratio n should be small.
- (b) Force ratio f should be large.

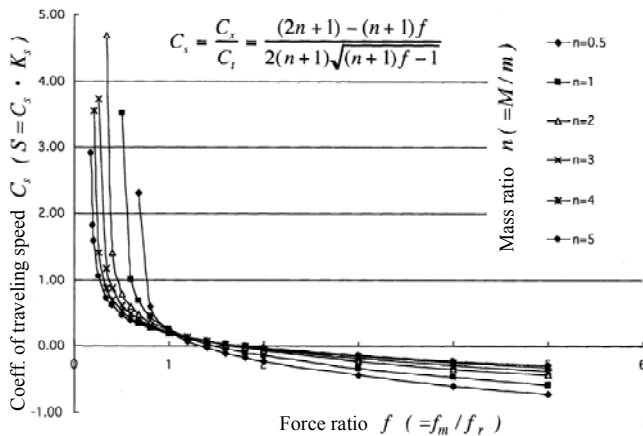


Fig. 5. Speed-force characteristics (calculation).

III. Experiments and results

Traveling tests

We made a traveling capsule as shown in Figs. 1 and 2. The capsule was put on the flat plastic plate and a step-shaped current was given to the coil. The capsule traveled exactly as we had predicted by theoretical analysis. The traveling speed measured in the experiment is shown in Fig. 6. As the voltage at the coil increased, which means higher magnetic force, the direction of travel changed and the speed characteristics were similar to the calculated result as shown in Fig. 5 above.

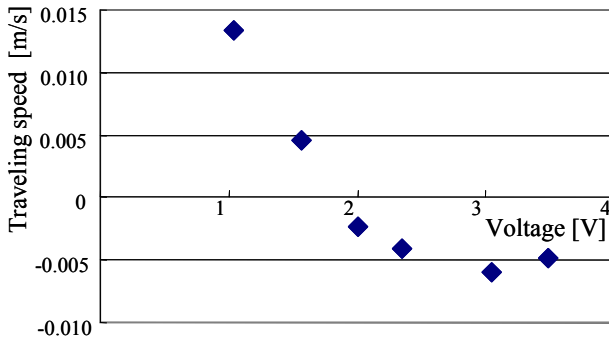


Fig. 6. Speed characteristics measured in the experiments. (capsule: aluminum, d = 7 mm, on dry plastic plate)

We tested making our capsule travel on the surface of a pig’s intestine. Although the speed of the capsule decreased to about half of that on the plastic plate, the capsule could also travel on the pig’s intestine.

Capsule surface temperature measurement

The capsule radiates heat while it is moving due to heat generated by current flowing through the coil. We measured the surface temperature of the capsule while it

was traveling, because the human body could be injured if the capsule surface is hot. Therefore, we made various types of capsule and measured the surface temperature to find which material and shape are good for preventing heat from leaving the capsule. The capsules we made are shown in Fig. 7. We chose aluminum, rubber, and acryl as the body material and compared their surface temperature when they were moving at the same speed. The temperature of a moving capsule was measured by an infra-red thermometer, which can measure temperature without touching the object. The results are shown in Table I. Capsule surface temperature did not increase much after 3 minutes of operation, so data for 3 minutes are shown in the table. The temperature at the surface of the capsules was always less than 37 °C. Among these capsules, a capsule with a large diameter has the advantage of relatively less power consumption and less heat: a thicker capsule has more space inside, and air in that space seemed to cut off the propagation of heat from the coil.

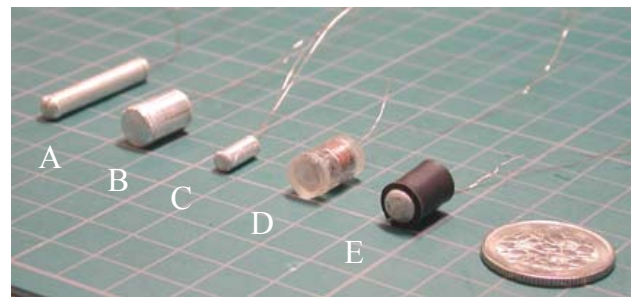


Fig. 7. Capsules made for comparison of heat.

Capsule	1 minute	2 minutes	3 minutes	Current	Voltage
A (l = 30 mm)	25.5 °C	25.8 °C	28.8 °C	0.55A	4.19V
B (d = 8 mm)	22.5 °C	22.5 °C	22.5 °C	0.12 A	1.22V
C (d = 4 mm)	22.0 °C	23.0 °C	23.3 °C	0.24 A	1.13V
D (acryl)	24.6 °C	25.1 °C	26.2 °C	0.09 A	0.91V
E (rubber)	27.3 °C	30.0 °C	35.5 °C	0.25 A	2.13V

Table I. Summary of capsule surface temperature measurements. (capsule speed: 10 mm/s, room temperature: 18 °C)

Friction force measurement

To use the results of the theoretical analysis and to improve the capsule traveling capability, it was necessary to measure the parameters of the actual capsule by experiments.

First, we measured friction force f_r between the capsule and a plate. For the plate material, plastic, rubber, and a phantom, which was a plastic material having similar elasticity characteristics to the living body, were chosen. The measurement setup is shown in Fig. 8 and the results are shown in Table II.

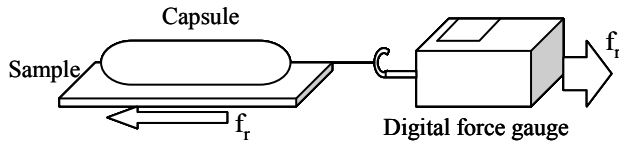


Fig. 8. Setup for measuring friction force f_r .

Capsule	Aluminum			
	Rubber plate	Phantom	Plastic plate	
Sample condition	Dry	Dry	Wet	Dry
Friction force f_r [N] (Average of 10 measured values)	0.020	0.015	0.018	0.005
Standard deviation	0.0034	0.0021	0.0016	0.0004

Table II. Summary of friction force measurements.

Magnetic force measurement

Also, magnetic force f_m was measured to fix the parameter. The measurement setup is shown in Fig. 9 and the results are shown in Fig. 10.

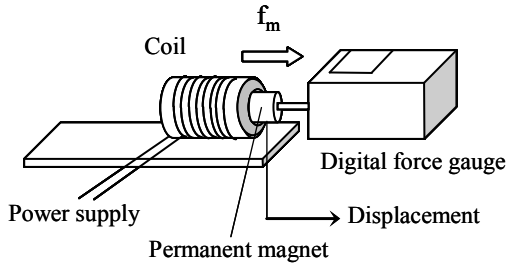


Fig. 9. Setup for measuring magnetic force f_m .

As shown in Fig. 10, within 4-mm displacement, the magnetic force increases depending on the displacement of the permanent magnet. Therefore, impact force at stopper A in Fig. 1 is bigger than that at stopper B. This asymmetric structure causes the capsule to travel in one direction.

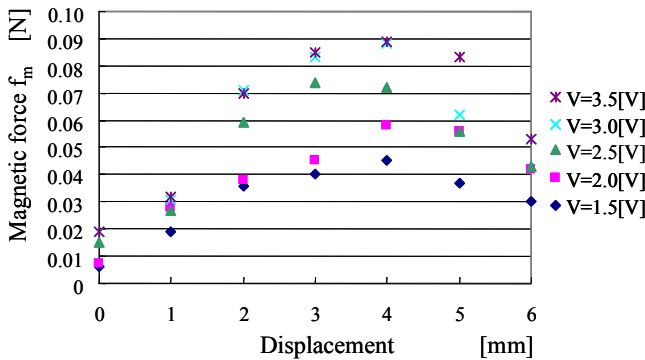


Fig. 10. Displacement-force characteristics.

The actual values of the parameters of our capsule were obtained as mentioned above. Using these parameters, the relation between the force ratio and speed was obtained as shown in Fig. 11. For the calculation, the go and return motion of the inner mass (permanent magnet) m is considered, as shown in Fig. 4. Speed S_T is defined by equation (25) using x_T and t_T . Coefficient of speed C_{ST} is expressed as equation (26). The value of returning magnetic force f_m' was set to be smaller than f_m according to the result shown in Fig. 10 above. Experimental results are also plotted in the figure. The results of both the experiment and the theory seem to coincide well.

$$S_T = \frac{x_T}{t_T} = \frac{-x_0 + x_1 + x_0' - x_1'}{t_0 + t_1 + t_0' + t_1'} \quad (25)$$

$$C_{ST} = \frac{S_T}{K_s}, \quad K_s = \sqrt{\frac{a \cdot f_r}{2M}}, \quad f_r' = f_r \quad (26)$$

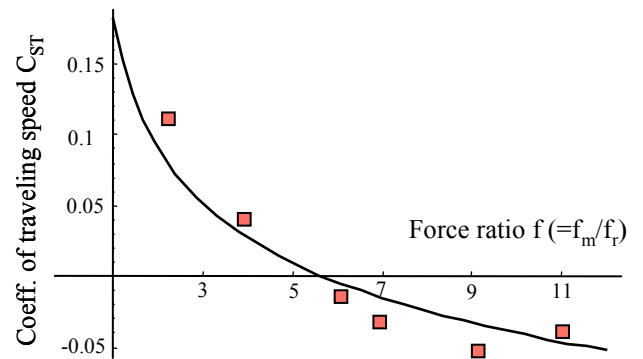


Fig. 11. Capsule speed characteristics (calculation) and experimental results, on a dry plastic plate.

Arranging the input signal for speedup

To make the capsule travel faster, we examined the theoretical analysis. We gave the capsule a standard rectangular input signal as shown in Fig. 12 (i). The capsule proceeded with to-and-fro vibration. Although the capsule moves forward, its backward motion is inefficient. The graph in Fig. 5 shows that the traveling direction changes as the force ratio increases. Therefore, the capsule can always proceed forward, if a greater input is given in the forward motion of the moving mass and a smaller input is given in the backward motion of the moving mass. The input signal shown in Fig. 12 (ii) was given to the capsule coil and the speed increased. The speed of the capsule with the proposed waveform (14 mm/s) was about twice as fast as that with the conventional waveform (6 mm/s).

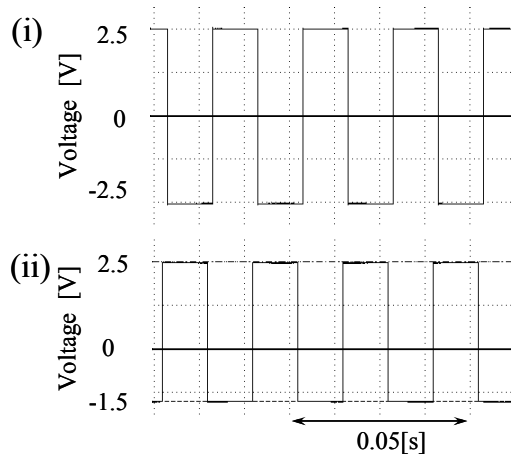


Fig. 12. Improvement of input voltage waveform:
(i) conventional; (ii) proposed.

- [10] Wakimoto, S., Suzumori, K., and Kanda, T., A Bio-mimetic Amphibious Soft Cord Robot, Transactions of The Japan Society of Mechanical Engineers, Series C, Vol. 72, No. 714, pp. 471-477, 2006.
- [11] Hirano, S., Luo, Zhi-Wei, and Kato, A., Development of An Inchworm-type Searching Robot, Journal of the Robotic Society of Japan, Vol. 24, No. 7, pp. 838-844, 2006.

IV. Conclusion

Even though the capsule has no wheels or legs, it can travel utilizing inertia force and friction force. We conducted theoretical analyses for the capsule and showed how the capsule mechanism worked. To increase capsule speed, a new input waveform was proposed and tested, proving that the new waveform approximately doubles the capsule speed compared with the conventional one. Our capsule may be useful for medical treatments such as inspection, drug delivery and operation.

Acknowledgement

This research was supported by a Grant-in-Aid for Scientific Research from the Japan Society for the Promotion of Science (#17560235).

References

- [1] Taylor, R. H., A Perspective on Medical Robotics, Proceedings of The IEEE, Vol. 94, No. 9, pp. 1652-1664, 2006.
- [2] Masuda N., Hayashi T., and Cai Y. Developments of Guidance Machine for Colonoscope, *Int. Journal of JSPE*, Vol. 28, No. 1, 1994.
- [3] Oura, M. and Hayashi T., Traveling machine with six legs for inside of tube, *Proc. of JSPE 1997 Spring Conference*, 1997.
- [4] Nakazato, Y., Ishii, T., Sato, H., and Ariga, Y., Development of In-pipe Mobile Robot Driven by Hydraulic Pressure, Proc. of The 3rd IFToMM Int. Micromechanism Symposium, pp. 13-16, 2001.
- [5] Takahashi, K., Japan Patent #H05-212093, 1992.
- [6] Adachi, H., Japan Patent #H06-154191, 1992.
- [7] Yoshida, K., Park, J.-H., Shimizu, T., and Yokota, S., A Micropump-Mounted In-Pipe Mobile Micromachine Using Homogeneous Electro-Rheological Fluid, Proc. of The 3rd IFToMM Int. Micromechanism Symposium, pp. 2-7, 2001.
- [8] Yokota, S., Functional Fluids from Point of View of Actuators, Journal of the Robotic Society of Japan, Vol. 24, No. 4, pp. 25-31, 2006.
- [9] Boyer, F., Porez, M., and Khalil, W., Macro-Continuous Computed Torque Algorithm for a Three-Dimensional Eel-Like Robot, IEEE Transactions on Robotics, Vol. 22, No. 4, pp. 763-775, 2006.